

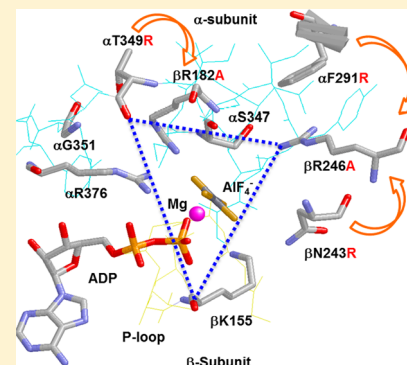
Significance of α Thr-349 in the Catalytic Sites of *Escherichia coli* ATP Synthase

Zulfiqar Ahmad,*[†] Mumeenat Winjobi,[†] and M. Anaul Kabir[‡]

[†]Department of Biochemistry, Kirksville College of Osteopathic Medicine, A. T. Still University of Health Sciences, Kirksville, Missouri 63501, United States

[‡]Molecular Genetics Laboratory, School of Biotechnology, National Institute of Technology, Calicut 673601, Kerala, India

ABSTRACT: This paper describes the role of α -subunit VISIT-DG sequence residue α Thr-349 in the catalytic sites of *Escherichia coli* F_1F_o ATP synthase. X-ray structures show the highly conserved α Thr-349 in the proximity (2.68 Å) of the conserved phosphate binding residue β R182 in the phosphate binding subdomain. α T349A, -D, -Q, and -R mutations caused 90–100-fold losses of oxidative phosphorylation and reduced ATPase activity of F_1F_o in membranes. Double mutation α T349R/ β R182A was able to partially compensate for the absence of known phosphate binding residue β R182. Azide, fluoroaluminate, and fluoroscandium caused insignificant inhibition of α T349A, -D, and -Q mutants, slight inhibition of the α T349R mutant, partial inhibition of the α T349R/ β R182A double mutant, and complete inhibition of the wild type. Whereas NBD-Cl (7-chloro-4-nitrobenzo-2-oxa-1,3-diazole) inhibited wild-type ATPase and its α T349A, -D, -R, and -Q mutants essentially completely, β R182A ATPase and double mutant α T349A/ β R182A were inhibited partially. Inhibition characteristics supported the conclusion that NBD-Cl reacts in β E (empty) catalytic sites, as shown previously by X-ray structure analysis. Phosphate protected against NBD-Cl inhibition in the wild type, α T349R, and double mutant α T349R/ β R182A but not in α T349A, α T349D, or α T349Q. The results demonstrate that α Thr-349 is a supplementary residue involved in phosphate binding and transition state stabilization in ATP synthase catalytic sites through its interaction with β R182.



In a 75 year life span, a typical 70 kg human generates approximately 2.0 million kg of ATP. The cell's energy currency is generated by converting food into useable energy by oxidation. F_1F_o ATP synthase is responsible for the fundamental means of cell energy production in animals, plants, and almost all microorganisms, which occurs by oxidation or photophosphorylation in membranes of bacteria, mitochondria, and chloroplasts. ATP synthase is one of the smallest biological nanomotors and is structurally similar in all species.^{1–4} In its simplest form, as in *Escherichia coli*, it contains eight different subunits distributed in the water-soluble F_1 sector (subunits $\alpha_3\beta_3\gamma\delta\epsilon$) and the membrane-associated F_o sector (subunits $a_2b_2c_{10}$). The total molecular size is ~530 kDa.⁴ In chloroplasts, there are two isoforms of subunit b. In mitochondria, there are seven to nine additional subunits, depending on the source, but in total, they contribute only a small fraction of additional mass and may have regulatory roles.^{5–7}

The membrane-bound F_1F_o ATP synthase enzyme is highly conserved and structurally identical among different species. X-ray structures of bovine enzyme⁸ established the presence of three catalytic sites at α -subunit– β -subunit interfaces of the $\alpha_3\beta_3$ hexamer. ATP hydrolysis and synthesis occur in the F_1 sector, whereas proton transport occurs through the membrane-embedded F_o .^{8,9} ATP synthesis is a result of proton gradient-driven clockwise rotation of γ (as viewed from the outer membrane), while ATP hydrolysis results in anticlockwise

rotation of the γ -subunit. Detailed reviews of ATP synthase structure and function may be found in refs 10–18.

A precise knowledge of P_i (inorganic phosphate) binding is not only essential for following the reaction mechanism of ATP synthesis and hydrolysis but also equally important for understanding the relationship between catalytic mechanism and mechanical rotation in this biological nanomotor. For this reason, we have focused our efforts on determining the role of conserved residues in and around catalytic site P_i binding subdomain.¹⁹ Knowledge of P_i binding residues and residues surrounding the P_i binding subdomain is imperative for (i) the molecular modulation of the catalytic site(s) for the improved catalytic and motor function of this enzyme, (ii) an explanation of how ATP synthase binds ADP and P_i within its catalytic sites in the face of a relatively high ATP/ADP concentration ratio, and (iii) understanding the relationship between P_i binding and subunit rotation.^{20–22} Many earlier attempts to measure P_i binding in purified *E. coli* F_1 failed to detect appreciable P_i binding at physiological P_i concentrations^{21,23,24} but modification of the assay devised by Perez et al.²⁵ provides a useful measure of P_i binding. In this assay, protection is afforded by P_i against inhibition of ATPase activity induced by covalent reaction with 7-chloro-4-nitrobenzo-2-oxa-1,3-diazole (NBD-

Received: September 19, 2014

Published: November 6, 2014

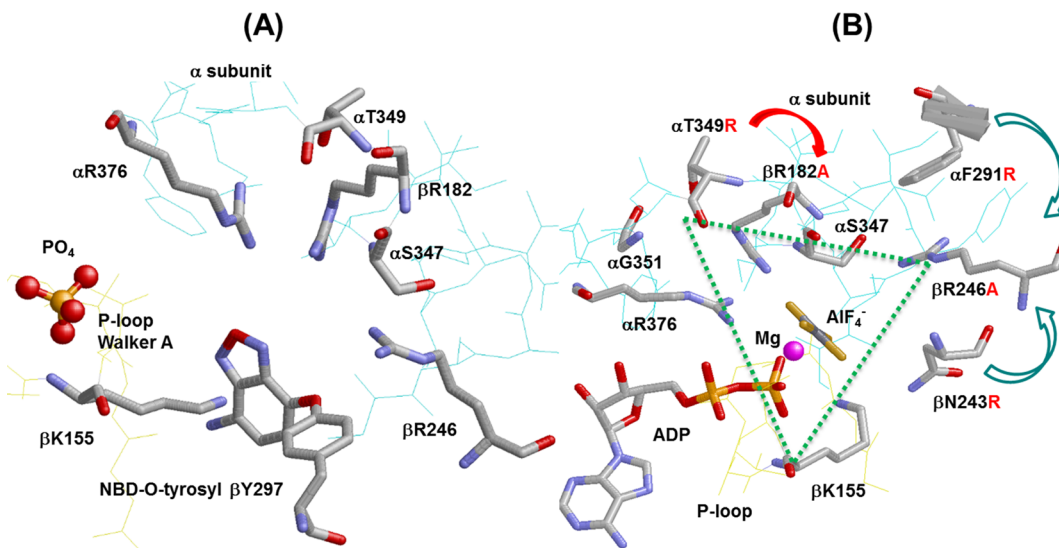


Figure 1. X-ray structures of catalytic sites in mitochondrial ATP synthase showing the spatial relationship of α -subunit VISIT-DG sequence residue α T349. (A) Reacted NBD-O-tyrosyl-297 in the β E site.²⁶ (B) β DP site in the AlF_4^- -inhibited enzyme.²⁸ *E. coli* residue numbering is shown. The dotted triangle shows residues β Lys-155, β Arg-182, β Arg-246, α Arg-376, α Ser-347, and α Thr-349 forming a triangular P_i binding site. Rasmol was used to generate these structures.

Cl). X-ray crystallography showed that the covalent interaction of NBD-Cl specifically with β 297 occurs in the β E catalytic site²⁶ (see Figure 1A); thus, protection afforded by P_i indicates that binding of P_i occurs at the β E catalytic site. Modification of the assay described above for *E. coli*, purified F_1 or $F_1\text{F}_o$ membranes, previously allowed us to investigate the relationship between P_i binding and catalysis for eight residues, namely, β Arg-246, β Asn-243, α Arg-376, β Lys-155, β Arg-182, α Phe-291, α Ser-347, and α Gly-351.^a Although all these residues are situated in the proximity of the phosphate analogues AlF_3 or SO_4^{2-} in X-ray structures of catalytic sites,^{27,28} we found that four residues, namely, β Arg-246, α Arg-376, β Lys-155, and β Arg-182, grouped in a triangular fashion, are directly involved in P_i binding while the fifth residue, α Ser-347, is indirectly involved in P_i binding through its interaction with β Arg-246 (see Figure 1B).^{19,29–35}

The mechanism of condensation of P_i with MgADP proposed by Senior et al.⁹ was strengthened by the X-ray crystallography structure of bovine ATP synthase of Menz et al.²⁸ showing the transition state analogue $\text{MgADP}\text{-AlF}_4^-$ trapped in catalytic sites (Figure 1B). It is clear from the geometry of this complex that the fluoroaluminate group occupies the position of the ATP γ -phosphate in the predicted transition state. The first transition state-like structure of F_1 from rat liver crystallized with the P_i analogue vanadate (V_i), reported by Pedersen's group, demonstrated that ADP was not essential, suggesting that the $\text{MgV}_i\text{-}F_1$ complex inhibited the catalytic activity to the same extent as that observed for the $\text{MgADP}\text{-V}_i\text{-}F_1$ complex.³⁶ Neither purified F_1 nor membrane-bound $F_1\text{F}_o$ from *E. coli* is inhibited by MgV_i or $\text{MgADP}\text{-V}_i$.³⁰ Consequently, we have relied on inhibition of ATPase activity by fluoroaluminate (or fluoroscandium) to assess the potential to stabilize a transition state complex.^{19,29–32,35}

Cingolani and Duncan¹⁸ have resolved the first *E. coli* F_1 sector high-resolution crystal structure in an autoinhibited conformation. This structure divulges a wealth of information about the regulatory features of bacterial and chloroplast ATP synthase. Moreover, the *E. coli* ATP synthase X-ray structure paves the way for the development of new antimicrobial drugs.

For *E. coli*, ATP synthase is naturally a better candidate for antimicrobial drugs in comparison to mitochondrial ATP synthase.^{4,18} Newly developed anti-tuberculosis drug targeting bacterial ATP synthase corroborates this assertion.³⁷ Because the *E. coli* high-resolution structure⁴ does not contain sulfate, phosphate, fluoroaluminate, or fluoroscandium, we have relied on the mitochondrial ATP synthase structure that is very similar to that of *E. coli* (~70% homologous sequence) as this study deals with the analogues described above.^{27,28,38}

Fortunately, by mutagenic analysis along with the NBD-Cl protection assay, as well as ATPase inhibition by transition state analogues, we can investigate the direct or indirect role of residues in P_i binding. In this work, we examine the role of the highly conserved α -subunit VISIT-DG sequence residue α Thr-349 in the process of P_i binding. Figure 1B shows the position of α Thr-349 with respect to other known P_i binding residues. The strategic position of α Thr-349 in the P_i binding subdomain leads to the following basic questions: Is α Thr-349 involved in P_i binding directly or indirectly? Do the α T349A, α T349D, α T349Q, and α T349R mutations have any effect on transition state formation? Also, can α T349R compensate for β Arg-182, a known P_i binding residue?

MATERIALS AND METHODS

Construction of Wild-Type and Mutant Strains of *E. coli*. The strain for wild-type *E. coli* was pBWU13.4/DK8.³⁹ All the mutants were generated by the method of Vandeyar et al.⁴⁰ The M13mp18 template containing the HindIII-XbaI fragment from plasmid pSN6 was used for oligonucleotide-directed mutagenesis. Plasmid pSN6 contains the β Y331W mutation from plasmid pSWM4⁴¹ introduced on a SacI-EagI fragment into pBWU13.4,³⁹ which expresses all the ATP synthase genes. The following mutagenic oligonucleotides were used: α T349A, GTAATCTCTATAAGCCGATGGTCAGATC, where the underlined bases introduce the mutation and a new SfcI restriction site; α T349D, GTAATCTCAATTGACGATGGTCAGATC, where the underlined bases introduce the mutation and a new MfeI restriction site; α T349Q, GTAATCTCCATTCAGGATGGTCAGATC, where the underlined base in-

troduces new mutation α T349Q (ACC → CAG); α T349R, CGTAATCTCCATTCGGGATGGTCAGATC, where the underlined bases introduce the mutation and a new NruI restriction site; β R182A, GGCGTAGGTGAAGCTACTCGT-GAGGG, where the underlined bases introduce the mutation and a new AluI restriction site. DNA sequencing was performed to confirm the presence of mutations and the absence of undesired changes in sequence, and the mutations were transferred to pSN6 on a Csp451 (an isoschizomer of BstBI) and the PmII fragment generating the new plasmids pZA20-(α T349A/ β Y331W), pZA21(α T349D/ β Y331W), pZA22-(α T349Q/ β Y331W), pZA23(α T349R/ β Y331W), and pZA24-(β R182A/ β Y331W). Double mutant pZA25 (α T349R/ β R182A) was generated by combining the pZA23 fragment on the pZA24 plasmid at the Csp451 and PmII site. Each plasmid was transformed into strain DK8⁴² containing a deletion of ATP synthase genes for expression of the mutant enzymes. It may be noted that all mutant strains contained the β Y331W mutation, which is valuable for measurement of nucleotide binding parameters⁴¹ and does not affect function significantly on its own. While the presence of the β Y331W mutation was not utilized in this work, the Trp mutation was included for possible future use.

Preparation of *E. coli* Membranes, Measurement of Growth Yield in Limiting Glucose Medium, and Assay of ATPase Activity of Membranes. *E. coli* membrane-bound F_1F_o were prepared by the method of Senior et al.⁴³ Notably in this procedure, F_1F_o -bound membrane initial pellets are washed three times. The first wash is conducted in buffer containing 50 mM TES (pH 7.0), 15% glycerol, 40 mM 6-aminohexanoic acid, and 5 mM *p*-aminobenzamidine. The next two washes are performed in buffer containing 5 mM TES (pH 7.0), 15% glycerol, 40 mM 6-aminohexanoic acid, 5 mM *p*-aminobenzamidine, 0.5 mM dithiothreitol (DTT), and 0.5 mM EDTA. Before the experiments, membranes were washed twice more by resuspension and ultracentrifugation in 50 mM TrisSO₄ (pH 8.0) and 2.5 mM MgSO₄. These extra washes are meant to reduce the null mutant to truly zero activity. Therefore, the low activities with the mutants must be coming from the mutants, not from any other contaminants. The experiments are performed to make sure that growth yield in limiting glucose was measured as described previously.⁴⁴ Measurement of ATPase activity was performed in 1 mL of assay buffer containing 10 mM NaATP, 4 mM MgCl₂, and 50 mM TrisSO₄ (pH 8.5) at 37 °C. Reactions were started by the addition of membrane-bound F_1F_o and stopped by addition of 1 mL of sodium dodecyl sulfate (SDS) to a final concentration of 3.3%. Release of P_i was measured as described in ref 45. Reaction times for the wild-type F_1F_o membrane (20–30 µg of protein) were 5–10 min, while reaction times for F_1F_o -bound mutant membranes (40–60 µg of protein) were 30–50 min. All reactions were found to be linear with time and protein concentration. The purity and integrity of membranes were checked by SDS gel electrophoresis on 10% acrylamide gels as described in ref 46 and immunoblotting with rabbit polyclonal anti- $F_1\alpha$ and anti- $F_1\beta$ antibodies as described in ref 47.

Inhibition of ATPase Activity by NBD-Cl and Protection by MgADP or P_i. A stock solution of NBD-Cl was prepared in dimethyl sulfoxide (DMSO) and protected from light. F_1F_o -bound membranes (0.2–0.5 mg/mL) were reacted with NBD-Cl for 60 min in the dark, at room temperature, in T8 [50 mM TrisSO₄ (pH 8.0)] and 2.5 mM MgSO₄. ATPase activity was determined by adding 50 µL

aliquots from the assay described above to 1 mL of ATPase assay buffer. For protection from NBD-Cl inhibition by ADP or P_i, membranes were preincubated for 60 min with a protecting agent at room temperature before the addition of NBD-Cl. MgSO₄ and ADP or P_i were present at equimolar concentrations in the reaction assay. Control samples containing the ligand without added NBD-Cl were included. Neither MgADP (up to 10 mM) nor P_i (up to 50 mM) had any inhibitory effect alone.

Reversal of NBD-Cl-Inhibited ATPase Activity by DTT.

To determine the DTT-induced reversal of NBD-Cl inhibition, F₁F_o-bound membranes were first reacted with NBD-Cl (150 µM) for 1 h at room temperature in the dark, and then DTT (final concentration of 4 mM) was added and incubation continued for 1 h at room temperature before the ATPase assay. Control samples without NBD-Cl and/or DTT were incubated for the same amounts of time.

Inhibition of ATPase Activity by Azide, Fluoroaluminate, or Fluoroscandium. For measurement of azide inhibition, membrane-bound F₁F_o was preincubated with varied concentrations of sodium azide for 30 min. Then 1 mL of ATPase assay buffer was added to measure the activity. Measurements of fluoroaluminate or fluoroscandium inhibition were performed by incubating membrane-bound F₁F_o for 60 min at room temperature in 50 mM TrisSO₄, 2.5 mM MgSO₄, 1 mM NaADP, and 10 mM NaF at a protein concentration of 0.2–0.5 mg/mL in the presence of varied concentrations of AlCl₃ or ScCl₃ (see Results); 50 µL aliquots were then added to 1 mL of ATPase assay buffer, and activity was measured as described above. It was confirmed in control experiments that no inhibition was seen if MgSO₄, NaADP, or NaF was omitted.

Inhibition of ATPase Activity by Dicyclohexylcarbodiimide (DCCD). The method of Weber et al.⁴⁸ was used to covalently modify the wild-type and mutant F₁F_o membrane by DCCD. Measurement of ATPase activity was done by adding 1 mL of ATPase assay buffer containing 10 mM NaATP, 4 mM MgCl₂, and 50 mM TrisSO₄ (pH 8.5) at 37 °C to the 100 µL aliquots of 16 h DCCD-modified ATP synthase.

RESULTS

Growth Properties of α T349A, α T349D, α T349Q, α T349R, β R182A, and α T349R/ β R182A Mutants of *E. coli* ATP Synthase. Five new single mutants, α T349A, α T349D, α T349Q, α T349R, and β R182A, and one double mutant, α T349R/ β R182A, were generated. Residue α Thr-349 was chosen for mutagenesis because of its high level of conservation in the α -subunit VISIT-DG sequence and proximity to the P_i binding pocket. The α T349A mutant was used to appreciate the role of the Thr-OH side chain in P_i binding and the transition state. The α T349Q mutant was designed to understand the impact of the larger side chain of Gln on α Thr-349. α T349D and α T349R were constructed to establish the impact of negative and positive charge on the nearby β R182, a known P_i binding residue. It should be noted here that the growth properties of β R182A were in excellent agreement with those published previously^{9,33} for the purified F₁ *E. coli* ATP synthase. The motivation behind double mutant α T349R/ β R182A was to determine if Arg on α T349 could compensate for the absence of Arg on β R182A.

Table 1 shows that introduction of Ala, Asp, Gln, or Arg as α T349A, α T349D, α T349Q, α T349R, and β R182A resulted in a loss of oxidative phosphorylation. All mutations barred growth on succinate-containing medium, and growth yields in

Table 1. Effects of α T349A, -D, -Q, and -R and α T349R/ β R182A Mutations on Cell Growth and ATPase Activity

species ^a	growth on succinate ^b	growth yield in limiting glucose (%)	ATPase activity ^c ($\mu\text{mol min}^{-1} \text{mg}^{-1}$)
wild type	++++	100	28
null	-	46	0
β Y331W	++++	95	26
α T349A	\pm	51	0.30
α T349D	\pm	49	0.28
α T349Q	\pm	47	0.29
α T349R	\pm	50	0.31
α T349R/ β R182A	++	66	4.40

^aWild type, pBWU13.4/DK8; null, pUC118/DK8. α T349A, -D, -Q, and -R and α T349R/ β R182A mutants were expressed with the β Y331W mutation also present, which does not significantly affect growth. Data are means of four to six experiments each. ^bGrowth on succinate plates after 3 days estimated by eye: +++, heavy growth; ++, substantial growth; \pm , very light growth; -, no growth. ^cATPase activity measured at 37 °C and expressed as micromoles of ATP hydrolyzed per minute per milligram of membrane protein. Each individual experimental point is itself the mean of duplicate assay tubes. Data are derived from two separate membrane preparations. Results from separate membrane preparations were in excellent agreement within $\pm 10\%$.

limiting glucose medium were reduced close to those of the ATP synthase null control. Substantial oxidative phosphorylation was retained by double mutant α T349R/ β R182A. Specific ATPase activities of membrane-bound F_1F_o preparations containing mutant enzymes were compared with wild-type and null control values, and the values are listed in Table 1. Mutations α T349A, α T349D, α T349Q, α T349R, and β R182A reduced the ATPase activity by 90–100-fold, while double mutant α T349R/ β R182A reduced ATPase activity ~6-fold. SDS gel electrophoresis and immunoblotting experiments yielded results that were in excellent agreement with previously published data and confirmed that the same amounts of α - and β -subunits were present in membrane-bound F_1F_o as in the wild type;^{19,29} therefore, reduced ATPase is not due to impaired assembly of ATP synthase or loss of F_1 during membrane preparation. Moreover, three extra washes reduce the activity of the null mutant to truly zero. Thus, the low mutant activities can be attributed only to mutant F_1 .

Inhibition of ATPase Activity of ATP Synthase in Membranes by NBD-Cl and Reversal by Dithiothreitol. All the inhibition assays were conducted using membrane-bound F_1F_o for both membrane preparations and the purified F_1 preparation, provide equivalent assay results, and are highly convenient and less time-consuming.^{19,29,30,35,49–52} Figure 2 shows NBD-Cl-induced inhibition of wild-type and mutant membranes in the presence of varied concentrations of NBD-Cl. NBD-Cl caused potent inhibition of the wild type with no residual activity, and this is consistent with previous studies.^{19,29–33,35} The α T349A mutant was also almost completely inhibited, while α T349D, α T349Q, α T349R, β R182A, and α T349R/ β R182A were inhibited by ~85, 90, 90, 60, and 50%, respectively, with ~10–50% residual activity. In previous studies, we have noted several instances in which mutant or wild-type ATP synthase was incompletely inhibited by inhibitors like fluoroaluminate, fluoros scandium, sodium azide, NBD-Cl, polyphenols, and peptides.^{19,29–33,35,49–52} To authenticate that maximal reaction with NBD-Cl had been

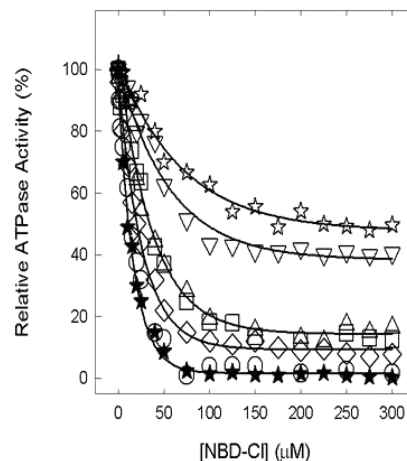


Figure 2. Inhibition of membrane-bound wild-type and mutant ATP synthase by NBD-Cl. Membranes were preincubated for 60 min at room temperature with varied concentrations of NBD-Cl; then aliquots were added to 1 mL of assay buffer, and ATPase activity was determined. Details are given in Materials and Methods. Symbols: (★) wild type, (○) α T349A, (□) α T349D, (◇) α T349Q, (△) α T349R, (▽) β R182A, and (☆) α T349R/ β R182A. Each data point represents an average of at least four experiments, using two or three independent membrane preparations of each mutant. Results agreed within $\pm 10\%$.

achieved, we incubated each membrane-bound F_1F_o preparation with 150 μM NBD-Cl for 1 h as in Figure 2, followed by a supplementary amount of 200 μM NBD-Cl (totaling 350 μM) and continuing the incubation for an extra hour before assaying ATPase activity. As expected, very little or no additional inhibition occurred (Figure 3A). This demonstrates that the reaction of NBD-Cl was complete and that fully reacted α T349D, α T349Q, α T349R, β R182A, and α T349R/ β R182A mutant F_1F_o membranes retained residual activity. Subsequently, we checked if inactivation by NBD-Cl could be reversed by addition of the reducing agent DTT because reversibility by DTT was indicative of specificity of reaction in previous studies. In this case, wild-type and mutant enzymes were preincubated with 150 μM NBD-Cl as in Figure 2 and then 4 mM DTT was added and incubation continued for 1 h before the ATPase assay. It can be seen in Figure 3B that DTT completely restored full activity in all cases. This proves that NBD-Cl reacts specifically with residue β Tyr-297 in the wild type as well as in six other mutants.^{53,54}

Protection against NBD-Cl Inhibition of ATPase Activity by MgADP or P_i . Panels A and B of Figure 4 show the MgADP protection data against NBD-Cl in wild-type and membrane-bound F_1F_o enzymes. It is seen that wild-type and mutant membranes were similarly protected against NBD-Cl inhibition. Earlier, we have shown that MgADP protects against NBD-Cl inhibition of wild-type soluble F_1 as well as membrane preparations of F_1F_o ; however, protection occurred only at high concentrations ($EC_{50} \sim 4.5$ mM MgADP). In this study, the EC_{50} values were 4.2, 3.1, 3.1, 4.4, 3.6, 2.5, and 4.8 mM for α T349A, α T349D, α T349Q, α T349R, β R182A, α T349R/ β R182A, and the wild type, respectively. We surmise that high concentrations are required to effectively keep the β E site occupied by MgADP in time average and thus hold back the access to NBD-Cl by sterically obstructing the site.^{19,29–35} This scheme is consistent with the conclusion of Orris et al.,²⁶ who provided X-ray crystallographic proof that NBD-Cl reacts specifically in the β E catalytic site. Therefore, we conclude that

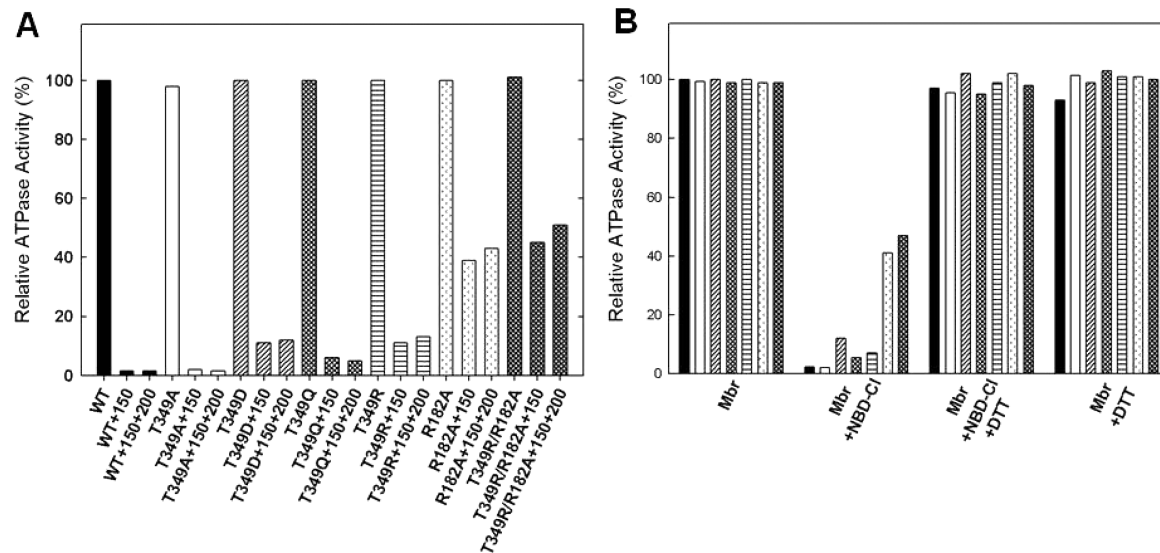


Figure 3. Results of an extra pulse of NBD-Cl in mutants and reversal of NBD-Cl effects by DTT. (A) Membrane ATP synthase (Mbr) was inhibited with 150 μ M NBD-Cl for 60 min under the conditions described in the legend of Figure 2. Then, a further pulse of 200 μ M NBD-Cl was added and incubation continued for 1 h before the assay. (B) Membrane ATP synthase (Mbr) was incubated with or without 150 μ M NBD-Cl for 60 min under the conditions described in the legend of Figure 2. The degree of inhibition was assayed. In parallel samples, 4 mM DTT was then added, and incubation was continued for a further 60 min before the assay. Each bar graph represents wild type, α T349A, α T349D, α T349Q, α T349R, β R182A, and α T349R/ β R182A from left to right.

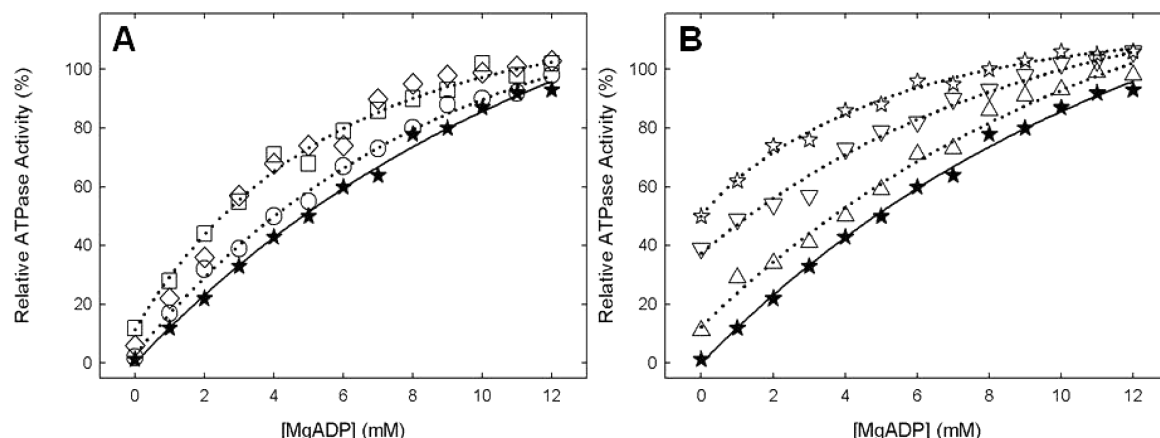


Figure 4. Protection against NBD-Cl reaction by MgADP. Wild-type and mutant membrane were preincubated for 1 h at room temperature with varied concentrations of MgADP as shown, and then 150 μ M NBD-Cl was added and incubation continued at room temperature in the dark for 1 h. Aliquots were then assayed for ATPase activity. Symbols: (★) wild type, (○) α T349A, (□) α T349D, (◇) α T349Q, (△) α T349R, (▽) β R182A, and (☆) α T349R/ β R182A. Results are means of quadruplicate experiments that agreed within $\pm 10\%$.

NBD-Cl is reacting in β E in the mutants and that the ATPase activities measured in the mutants can be attributed to the ATP synthase enzyme and not to a contaminant.

Figure 5 shows the MgP_i protection against the NBD-Cl reaction. It is obvious that P_i protected well against NBD-Cl inhibition of ATPase activity in the wild type, α T349R, and α T349R/ β R182A but did not protect at all against NBD-Cl inactivation in α T349A, α T349D, α T349Q, or β R182A.

Inhibition of ATPase Activity by Fluoroaluminate, Fluoroscandium, and Azide. Subsequently, we examined the effects of transition state and ground state analogues. Panels A and B of Figure 6 show inhibition of wild-type and mutant enzymes by MgADP-fluoroaluminate and MgADP-fluoroscandium, respectively. The wild type was completely inhibited. Levels of AlF_x⁻ and ScF_x⁻induced inhibition of mutants were ~25 and 32% (α T349A), 5 and 12% (α T349D), 49 and 46% (α T349R), 17 and 22% (β R182A), and 65 and 61% (α T349R/

β R182A), respectively. In contrast, mutant α T349Q was particularly resistant to inhibition by either MgADP-fluoroaluminate or MgADP-fluoroscandium. Figure 6C shows that azide, another potent inhibitor of ATPase in ATP synthase, strongly inhibited the wild type but showed varied residual activity of ~53% (α T349A), ~90% (α T349D), ~90% (α T349Q), ~40% (α T349R), ~72% (β R182A), and ~21% (α T349R/ β R182A) in mutants.

Inhibition of ATPase Activity by DCCD. Figure 7 shows the wild-type, α T349A, α T349D, α T349Q, α T349R, β R182A, and α T349R/ β R182A enzymes inactivated by DCCD. While the wild type is completely inhibited by 200 μ M DCCD after incubation for 16 h at room temperature, mutants show varied degrees of inhibition. α T349A is inhibited ~31%, α T349Q ~7%, α T349R ~43%, β R182A ~19%, and α T349R/ β R182A ~72%, while α T349D is not inhibited at all. In another set of experiments with 2 or 5 h incubations using the same DCCD

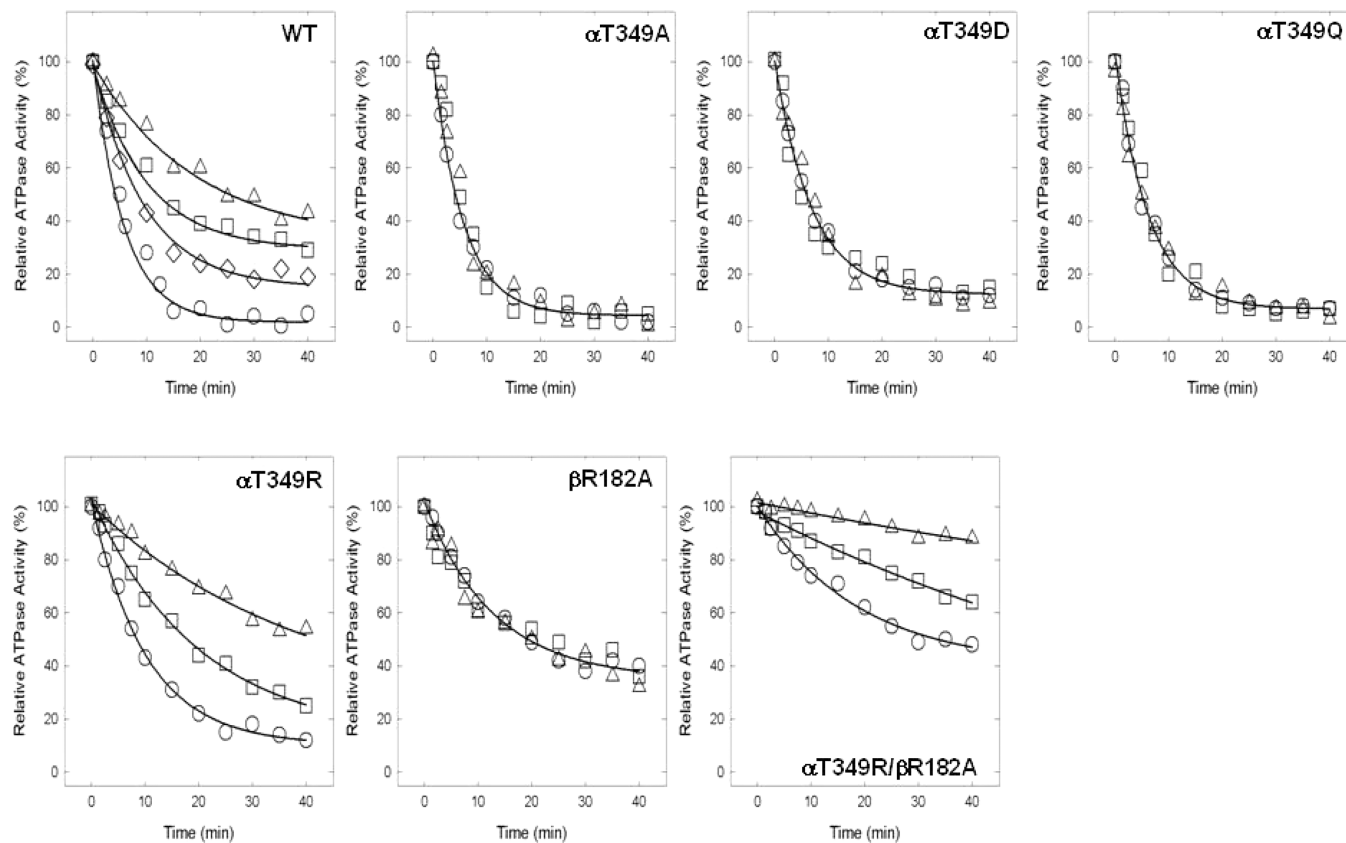


Figure 5. Protection by P_i of ATPase activity in wild-type and mutant membranes from inactivation by NBD-Cl. Membranes were preincubated with MgP_i at 0, 2.5, 5, or 10 mM as shown, for 60 min at room temperature. Then NBD-Cl (150 μ M) was added, and aliquots were withdrawn for the assay at time intervals as shown. The ATPase activity remaining is plotted vs time of incubation with NBD-Cl: (○) no P_i added, (◊) 2.5 mM P_i , (□) 5 mM P_i , and (△) 10 mM P_i . Each data point represents the average of four different experiments using two or three independent membrane preparations of each mutant.

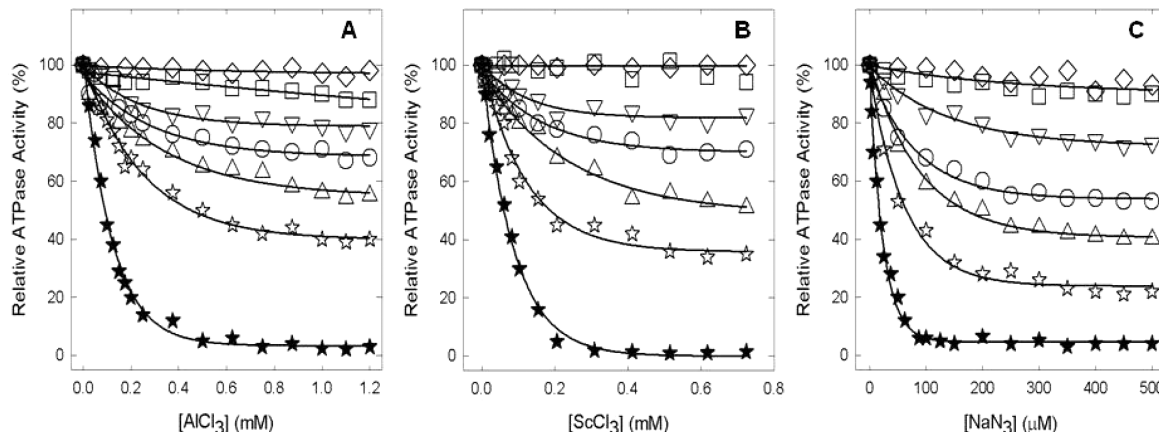


Figure 6. Inhibition of membrane ATPase activity from mutant and wild-type ATP synthase enzymes by fluoroaluminate, fluoroscandium, and azide. Membranes were preincubated for 60 min at room temperature with 1 mM MgADP, 10 mM NaF, and the indicated concentration of $AlCl_3$ (A) or $ScCl_3$ (B). Then aliquots were added to 1 mL of assay buffer, and ATPase activity was determined. Sodium azide was added directly to the membranes and incubated for 30 min before the assay (C) (for details, see Materials and Methods). Symbols: (★) wild type, (○) α T349A, (□) α T349D, (◊) α T349Q, (△) α T349R, (▽) β R182A, and (☆) α T349R/βR182A. All the data points are means of at least four different experiments using two or three independent membrane preparations of each mutant. The variation was $\pm 10\%$ between different experiments.

concentrations and reaction conditions, we found that the wild type was still fully inhibited, α T349A, α T349D, α T349Q, α T349R, and β R182A showed no inhibition, but double mutant α T349R/βR182A was inhibited maximally by 25% (2 h) and 55% (5 h).

DISCUSSION

The objective of this study was to examine the functional role(s) of residue α -Thr-349 of *E. coli* ATP synthase. This residue is part of the strongly conserved α -subunit VISIT-DG sequence. The VISIT-DG sequence residues are located in the proximity of the α -subunit– β -subunit interface bordering the P_i

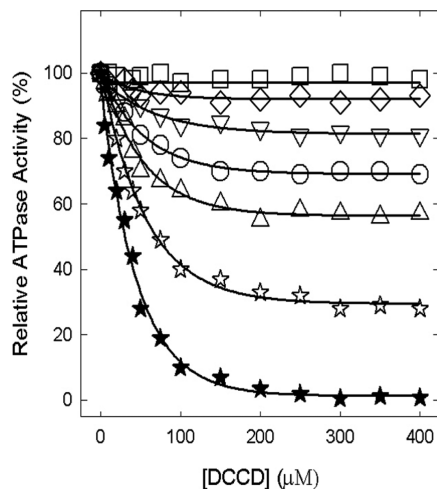


Figure 7. Inhibition of membrane ATPase activity from mutant and wild-type ATP synthase enzymes by DCCD. Membranes were preincubated for 16 h at room temperature with the varied concentrations of DCCD indicated in the figure. Then 1 mL of ATPase assay buffer was added to determine the activity. Symbols: (★) wild type, (○) α T349A, (□) α T349D, (◇) α T349Q, (△) α T349R, (▽) β R182A, and (☆) α T349R/ β R182A. All the data points are means of at least four different experiments using two or three independent membrane preparations of each mutant. The variation was $\pm 10\%$ between different experiments.

binding pocket (Figure 1B). X-ray crystal structures of the AlF_3 -inhibited enzyme²⁷ as well as the AlF_4^- -inhibited enzyme (which also contained SO_4^{2-} in a second catalytic site)²⁸ show that the side chain of residue α Thr-349 is very close to these bound P_i analogues (Figure 1). P_i binding is fundamental for ATP synthesis by ATP synthase. Therefore, the process of P_i binding can divulge a wealth of information about ATP synthesis. Mutagenic analysis and molecular modulation of P_i binding residues are some of the best ways to examine and appreciate the functional role of residues in the catalytic site.

Earlier studies established that mutagenesis combined with the use of the P_i protection assay against NBD-Cl inhibition, as well as the use of inhibitory analogues, allowed the characterization of functional role(s) of residues suspected to be involved in P_i binding.^{19,29–35} From analysis of eight such catalytic site residues, we determined that five residues, namely, α Arg-376, β Arg-182, β Arg-246, β Lys-155, and α Ser-347, are critical for P_i binding and form a triangular subdomain within the catalytic site. While four residues, α Arg-376, β Arg-182, β Arg-246, and β Lys-155, were directly involved in P_i binding, the fifth residue, α Ser-347, supported P_i binding and transition state stabilization through its interaction with β Arg-246 (and possibly with β Arg-182, too)^{19,29–35} (Figure 1B). Earlier, we also established that introduction of negative or positive charge at this location resulted in strong alteration of P_i binding,^{29,31,35} indicating that negative charge within the triangular subdomain was an important determinant of P_i binding. Here we used the same approaches to study the α Thr-349 residue.

Generation of the α T349A, α T349D, α T349Q, α T349R, β R182A, or α T349R/ β R182A mutant did not affect the assembly or structural integrity of the membrane ATP synthase. Membrane-bound F_1F_o showed similar contents of F_1 α - and β -subunits compared to the wild type. The α T349A, α T349D, α T349Q, or β R182A mutation caused severe loss of oxidative phosphorylation as judged by growth on succinate or limiting

glucose medium. Also, strong inhibition of ATPase activity was observed along with abrogation of P_i binding. The α T349R/ β R182A double mutant allowed P_i binding with substantial oxidative phosphorylation and ATPase activity. The α T349R mutant was interesting for it has very little ATPase activity with no oxidative phosphorylation and still allowed P_i binding just like double mutant α T349R/ β R182A (Table 1 and Figure 5).

Fluoroaluminate and fluoroscandium in combination with MgADP potently inhibit wild-type *E. coli* ATP synthase,^{19,29–33,35,55,56} and both are believed to mimic the chemical transition state. Transition state-like structures involving the bound MgADP- AlF_4^- complex have been seen in catalytic sites in ATP synthase by X-ray crystallography.²⁸ MgADP-fluoroaluminate or MgADP-fluoroscandium failed to inhibit α T349D and α T349Q mutants, indicating strong destabilization of the transition state, while partial inhibition occurred in α T349A, and β Arg-182, α T349R, and double mutant α T349R/ β R182A, representative of the partial destabilization of the transition state (Figure 6A,B). These results are in agreement with the amount of oxidative phosphorylation and ATPase activity found in each of the mutants. Evidently, α -subunit VISIT-DG sequence residue α Thr-349 is involved directly in the transition state and in catalysis and therefore should be considered as a sixth member of the group of P_i binding residues that make up the triangular P_i binding pocket.

All mutations affected the degree of inhibition by azide, with double mutant α T349R/ β R182A reducing it substantially (by $\sim 80\%$) and α T349A ($\sim 47\%$), α T349D ($\sim 10\%$), α T349Q ($\sim 10\%$), α T349R ($\sim 60\%$), and β R182A ($\sim 28\%$) reducing it less severely (Figure 6C). An X-ray crystallographic study of azide-induced inhibition of ATP hydrolysis⁵⁷ showed that azide inhibits ATP synthase by forming a tight binding MgADP-azide complex in β DP catalytic sites, which resembles that formed by MgADP-beryllium fluoride, and may therefore be considered an analogue of the MgATP ground state. In the MgADP-azide complex, the azide occupies a position equivalent to that of the γ -phosphate of MgATP. Thus, all mutants also had effects on substrate binding by virtue of an effect at the γ -P position.

DCCD inhibits wild-type *E. coli* F_1 by reacting with residue β Glu-192⁵⁸ and/or cAsp-61,⁵⁹ with the latter predominating at lower DCCD concentrations and/or shorter incubation times. As expected, wild-type ATP synthase was inhibited almost 100%. The α T349D mutant was not inhibited at all, and α T349A was inhibited $\sim 30\%$, α T349Q $\sim 7\%$, α T349R $\sim 43\%$, β Arg-182 $\sim 20\%$, and double mutant α T349R/ β Arg-182 $\sim 72\%$ (Figure 7). Notably, at shorter incubation times, while double mutant α T349R/ β Arg-182 showed substantial inhibition, all the single mutations resisted inhibition (see Results). The data therefore indicate that in the α T349R/ β Arg-182 double mutant ATPase activity on F_1 is partly coupled to proton translocation in F_o , which explains why double mutant α T349R/ β Arg-182 retains some growth on succinate and in limiting glucose (Table 1).

It is interesting to note here that P_i binding and release events have been shown to be directly linked to rotation of the central stalk in single-molecule experiments.⁶⁰ Perturbation of the P_i binding site might well be anticipated to perturb the integrity of the link between P_i binding and rotation and manifest as uncoupling. Thus, the data for the α Thr-349 mutation strongly suggest that the Thr-OH group is needed for transition state stabilization and P_i binding.

It is established that Arg residues occur frequently in P_i binding sites in proteins,³⁰ therefore, varying the number of Arg residues in the P_i binding site of ATP synthase seemed to be a useful approach. Residue α Thr-349 lies 2.68 and 4.38 Å, 2.86 and 4.01 Å, and 3.61 and 3.40 Å from known P_i binding residues β Arg-182 and α Arg-376, respectively, in AlF₃⁻, AlF₄⁻, and SO₄²⁻-containing catalytic sites (nearest atom distances). Thus, one experimental approach we used was to introduce mutation α T349R into the wild-type background (with β Arg-182) in the presence of the β R182A mutation. The location of residue α Thr-349 at the end of the P_i binding pocket across the catalytic α -subunit– β -subunit interface with its side chain pointing toward the bound P_i analogues also appeared to be a suitable location for the introduction of a new Arg. Apparently, the α T349R mutation would place extra positive charge relatively close to P_i, and double mutation α T349R/ β R182A will allow the α T349R mutant Arg to fit into the large “hole” generated by the β Ala-182 mutation. The β R182A mutant did not show P_i binding, but the α T349R mutation “rescued” P_i binding in combination with β R182A (Figure 5). On the basis of the loss of oxidative phosphorylation that was made evident by growth on succinate or limiting glucose medium along with very low ATPase activity, α Arg-349 could be expected to assume the same exact stereochemical interactions achieved by β Arg-182. Thus, electrostatic interaction per se is therefore important, and we conclude that the presence of at least one positive charge at this general location is a requisite determinant of initial P_i binding in catalytic site β E. In addition, the α T349R mutation in the wild-type background totaling one extra positive charge did not prevent P_i binding (Figure 5), but the presence of negative charge in the form of α T349D resulted in abrogation of P_i binding. Presumably, the presence of Asp negated the positive charge of nearby residue β Arg-182, resulting in the abrogation of P_i binding.

α Thr-349 is positioned close to bound AlF₄⁻ in catalytic sites (see Figure 1B).²⁸ The Thr-OH lies 5.46 Å from the F3 atom in AlF₄⁻ and thus may contribute to transition state stabilization by direct interaction. It may be mentioned that a similar conclusion was reached regarding the -OH group contributed by α Ser-347 of the *E. coli* VISIT-DG sequence¹⁹ and Ser-OH of the highly conserved “LSGGQ” ABC signature sequence in P-glycoprotein.⁶¹ Considering how P_i binding is affected, α Thr-349-OH lies 6.44 Å from O2 in SO₄²⁻²⁸ and 5.56 Å from F1 of AlF₃ in the respective catalytic sites.²⁷ Thus, some direct interaction may be operative. However, more important than the findings described above may be the fact that the Thr-OH lies 2.86 Å from NH2 of β Arg-182 (in the AlF₄⁻ site) and 2.68 Å from NH2 of β Arg-182 in the AlF₃-occupied site. β Arg-182 is strongly conserved and critical for P_i binding and transition state stabilization.^{9,33} Further, the carbonyl O of α Thr-349 lies 3.40 and 3.63 Å from NH1 and NH2, respectively, of α Arg-376, another P_i binding residue. The likely H-bond interaction between α Thr-349 and β Arg-182 (and α Arg-376) suggests these residues act together to support P_i binding and transition state stabilization.

In summary, the α Thr-349 residue of the conserved VISIT-DG sequence in the ATP synthase α -subunit is required for catalysis, P_i binding, and transition state stabilization. Introduction of Arg at this site can compensate for the absence of Arg at the known P_i binding residue β Arg-182 site. Furthermore, arrangement of positive charges with respect to one another is of paramount importance for oxidative phosphorylation and P_i binding.

AUTHOR INFORMATION

Corresponding Author

*Department of Biochemistry, Kirksville College of Osteopathic Medicine, A. T. Still University of Health Sciences, Kirksville, MO 63501. E-mail: zahmad@atsu.edu. Phone: (660) 626-2144.

Funding

This work was supported by National Institutes of Health Grant GM085771 to Z.A.

Notes

The authors declare no competing financial interest.

ACKNOWLEDGMENTS

We are thankful to Dr. Alan Senior (Professor Emeritus, Department of Biochemistry and Biophysics, University of Rochester Medical Center, Rochester, NY) for his suggestions and comments on the manuscript.

ADDITIONAL NOTE

E. coli residue numbering used throughout.

REFERENCES

- (1) Senior, A. E. (2012) Two ATPases. *J. Biol. Chem.* 287, 30049–30062.
- (2) Ahmad, Z., and Cox, J. L. (2014) ATP Synthase: The Right Size Base Model for Nanomotors in Nanomedicine. *Sci. World J.* 2014, 10.
- (3) Wada, Y., Sambongi, Y., and Futai, M. (2000) Biological nano motor, ATP synthase F_oF₁: From catalysis to γ ec(10–12) subunit assembly rotation. *Biochim. Biophys. Acta* 1459, 499–505.
- (4) Roy, A., Hutcheon, M. L., Duncan, T. M., and Cingolani, G. (2012) Improved crystallization of *Escherichia coli* ATP synthase catalytic complex (F1) by introducing a phosphomimetic mutation in subunit e. *Acta Crystallogr. F*68, 1229–1233.
- (5) Senior, A. E. (1988) ATP synthesis by oxidative phosphorylation. *Physiol. Rev.* 68, 177–231.
- (6) Karrasch, S., and Walker, J. E. (1999) Novel features in the structure of bovine ATP synthase. *J. Mol. Biol.* 290, 379–384.
- (7) Devenish, R. J., Prescott, M., Roucou, X., and Nagley, P. (2000) Insights into ATP synthase assembly and function through the molecular genetic manipulation of subunits of the yeast mitochondrial enzyme complex. *Biochim. Biophys. Acta* 1458, 428–442.
- (8) Abrahams, J. P., Leslie, A. G. W., Lutter, R., and Walker, J. E. (1994) Structure at 2.8 Å resolution of F1-ATPase from bovine heart mitochondria. *Nature* 370, 621–628.
- (9) Senior, A. E., Nadanaciva, S., and Weber, J. (2002) The molecular mechanism of ATP synthesis by F1F0-ATP synthase. *Biochim. Biophys. Acta* 1553, 188–211.
- (10) Noji, H., and Yoshida, M. (2001) The rotary machine in the cell, ATP synthase. *J. Biol. Chem.* 276, 1665–1668.
- (11) Weber, J., and Senior, A. E. (2003) ATP synthesis driven by proton transport in F1F0-ATP synthase. *FEBS Lett.* 545, 61–70.
- (12) Frasch, W. D. (2000) The participation of metals in the mechanism of the F₁-ATPase. *Biochim. Biophys. Acta* 1458, 310–325.
- (13) Pedersen, P. L. (2007) Transport ATPases into the year 2008: A brief overview related to types, structures, functions and roles in health and disease. *J. Bioenerg. Biomembr.* 39, 349–355.
- (14) Ahmad, Z., Okafor, F., and Laughlin, T. F. (2011) Role of Charged Residues in the Catalytic Sites of *Escherichia coli* ATP Synthase. *J. Amino Acids* 2011, 785741.
- (15) Ahmad, Z., and Laughlin, T. F. (2010) Medicinal chemistry of ATP synthase: A potential drug target of dietary polyphenols and amphibian antimicrobial peptides. *Curr. Med. Chem.* 17, 2822–2836.
- (16) Senior, A. E. (2007) ATP synthase: Motoring to the finish line. *Cell* 130, 220–221.

- (17) Martin, J. L., Ishmukhametov, R., Hornung, T., Ahmad, Z., and Frasch, W. D. (2014) Anatomy of F1-ATPase powered rotation. *Proc. Natl. Acad. Sci. U.S.A.* **111**, 3715–3720.
- (18) Cingolani, G., and Duncan, T. M. (2011) Structure of the ATP synthase catalytic complex (F(1)) from *Escherichia coli* in an autoinhibited conformation. *Nat. Struct. Mol. Biol.* **18**, 701–707.
- (19) Li, W., Brudecki, L. E., Senior, A. E., and Ahmad, Z. (2009) Role of α -subunit VISIT-DG sequence residues Ser-347 and Gly-351 in the catalytic sites of *Escherichia coli* ATP synthase. *J. Biol. Chem.* **284**, 10747–10754.
- (20) Boyer, P. D. (1989) A perspective of the binding change mechanism for ATP synthesis. *FASEB J.* **3**, 2164–2178.
- (21) al-Shawi, M. K., and Senior, A. E. (1992) Effects of dimethyl sulfoxide on catalysis in *Escherichia coli* F1-ATPase. *Biochemistry* **31**, 886–891.
- (22) Al-Shawi, M. K., Ketchum, C. J., and Nakamoto, R. K. (1997) The *Escherichia coli* FOF1 γ M23K uncoupling mutant has a higher K0.5 for Pi. Transition state analysis of this mutant and others reveals that synthesis and hydrolysis utilize the same kinetic pathway. *Biochemistry* **36**, 12961–12969.
- (23) Lobau, S., Weber, J., and Senior, A. E. (1998) Catalytic site nucleotide binding and hydrolysis in F1FO-ATP synthase. *Biochemistry* **37**, 10846–10853.
- (24) Weber, J., and Senior, A. E. (1995) Location and properties of pyrophosphate-binding sites in *Escherichia coli* F1-ATPase. *J. Biol. Chem.* **270**, 12653–12658.
- (25) Perez, J. A., Greenfield, A. J., Sutton, R., and Ferguson, S. J. (1986) Characterisation of phosphate binding to mitochondrial and bacterial membrane-bound ATP synthase by studies of inhibition with 4-chloro-7-nitrobenzofuran. *FEBS Lett.* **198**, 113–118.
- (26) Orriss, G. L., Leslie, A. G., Braig, K., and Walker, J. E. (1998) Bovine F1-ATPase covalently inhibited with 4-chloro-7-nitrobenzofuran: The structure provides further support for a rotary catalytic mechanism. *Structure* **6**, 831–837.
- (27) Braig, K., Menz, R. I., Montgomery, M. G., Leslie, A. G., and Walker, J. E. (2000) Structure of bovine mitochondrial F₁-ATPase inhibited by Mg²⁺ADP and aluminium fluoride. *Structure* **8**, 567–573.
- (28) Menz, R. I., Walker, J. E., and Leslie, A. G. (2001) Structure of bovine mitochondrial F₁-ATPase with nucleotide bound to all three catalytic sites: Implications for the mechanism of rotary catalysis. *Cell* **106**, 331–341.
- (29) Ahmad, Z., and Senior, A. E. (2005) Modulation of charge in the phosphate binding site of *Escherichia coli* ATP synthase. *J. Biol. Chem.* **280**, 27981–27989.
- (30) Ahmad, Z., and Senior, A. E. (2004) Mutagenesis of residue β Arg-246 in the phosphate-binding subdomain of catalytic sites of *Escherichia coli* F1-ATPase. *J. Biol. Chem.* **279**, 31505–31513.
- (31) Ahmad, Z., and Senior, A. E. (2004) Role of β Asn-243 in the phosphate-binding subdomain of catalytic sites of *Escherichia coli* F₁-ATPase. *J. Biol. Chem.* **279**, 46057–46064.
- (32) Ahmad, Z., and Senior, A. E. (2005) Identification of phosphate binding residues of *Escherichia coli* ATP synthase. *J. Bioenerg. Biomembr.* **37**, 437–440.
- (33) Ahmad, Z., and Senior, A. E. (2005) Involvement of ATP synthase residues α Arg-376, β Arg-182, and β Lys-155 in Pi binding. *FEBS Lett.* **579**, 523–528.
- (34) Ahmad, Z., and Senior, A. E. (2006) Inhibition of the ATPase activity of *Escherichia coli* ATP synthase by magnesium fluoride. *FEBS Lett.* **580**, 517–520.
- (35) Brudecki, L. E., Grindstaff, J. J., and Ahmad, Z. (2008) Role of α Phe-291 residue in the phosphate-binding subdomain of catalytic sites of *Escherichia coli* ATP synthase. *Arch. Biochem. Biophys.* **471**, 168–175.
- (36) Chen, C., Saxena, A. K., Simcocke, W. N., Garboczi, D. N., Pedersen, P. L., and Ko, Y. H. (2006) Mitochondrial ATP synthase. Crystal structure of the catalytic F1 unit in a vanadate-induced transition-like state and implications for mechanism. *J. Biol. Chem.* **281**, 13777–13783.
- (37) Andries, K., Verhasselt, P., Guillemont, J., Gohlmann, H. W., Neefs, J. M., Winkler, H., Van Gestel, J., Timmerman, P., Zhu, M., Lee, E., Williams, P., de Chaffoy, D., Huitric, E., Hoffner, S., Cambau, E., Truffot-Pernot, C., Lounis, N., and Jarlier, V. (2005) A diarylquinoline drug active on the ATP synthase of *Mycobacterium tuberculosis*. *Science* **307**, 223–227.
- (38) Walker, J. E., Saraste, M., Runswick, M. J., and Gay, N. J. (1982) Distantly related sequences in the α - and β -subunits of ATP synthase, myosin, kinases and other ATP-requiring enzymes and a common nucleotide binding fold. *EMBO J.* **1**, 945–951.
- (39) Ketchum, C. J., Al-Shawi, M. K., and Nakamoto, R. K. (1998) Intergenic suppression of the γ M23K uncoupling mutation in FOF1 ATP synthase by β Glu-381 substitutions: The role of the β 380DEL-SEED386 segment in energy coupling. *Biochem. J.* **330**, 707–712.
- (40) Vandeyar, M. A., Weiner, M. P., Hutton, C. J., and Batt, C. A. (1988) A simple and rapid method for the selection of oligodeoxynucleotide-directed mutants. *Gene* **65**, 129–133.
- (41) Weber, J., Wilke-Mounts, S., Lee, R. S., Grell, E., and Senior, A. E. (1993) Specific placement of tryptophan in the catalytic sites of *Escherichia coli* F1-ATPase provides a direct probe of nucleotide binding: Maximal ATP hydrolysis occurs with three sites occupied. *J. Biol. Chem.* **268**, 20126–20133.
- (42) Klionsky, D. J., Brusilow, W. S., and Simoni, R. D. (1984) In vivo evidence for the role of the ϵ subunit as an inhibitor of the proton-translocating ATPase of *Escherichia coli*. *J. Bacteriol.* **160**, 1055–1060.
- (43) Senior, A. E., Langman, L., Cox, G. B., and Gibson, F. (1983) Oxidative phosphorylation in *Escherichia coli*. Characterization of mutant strains in which F1-ATPase contains abnormal β -subunits. *Biochem. J.* **210**, 395–403.
- (44) Senior, A. E., Latchney, L. R., Ferguson, A. M., and Wise, J. G. (1984) Purification of F1-ATPase with impaired catalytic activity from partial revertants of *Escherichia coli* uncA mutant strains. *Arch. Biochem. Biophys.* **228**, 49–53.
- (45) Taussky, H. H., and Shorr, E. (1953) A microcolorimetric method for the determination of inorganic phosphorus. *J. Biol. Chem.* **202**, 675–685.
- (46) Laemmli, U. K. (1970) Cleavage of structural proteins during the assembly of the head of bacteriophage T4. *Nature* **227**, 680–685.
- (47) Rao, R., Perlin, D. S., and Senior, A. E. (1987) The defective proton-ATPase of uncA mutants of *Escherichia coli*: ATP-binding and ATP-induced conformational change in mutant α -subunits. *Arch. Biochem. Biophys.* **255**, 309–315.
- (48) Weber, J., Wilke-Mounts, S., and Senior, A. E. (1994) Cooperativity and stoichiometry of substrate binding to the catalytic sites of *Escherichia coli* F1-ATPase. Effects of magnesium, inhibitors, and mutation. *J. Biol. Chem.* **269**, 20462–20467.
- (49) Chinnam, N., Dadi, P. K., Sabri, S. A., Ahmad, M., Kabir, M. A., and Ahmad, Z. (2010) Dietary bioflavonoids inhibit *Escherichia coli* ATP synthase in a differential manner. *Int. J. Biol. Macromol.* **46**, 478–486.
- (50) Dadi, P. K., Ahmad, M., and Ahmad, Z. (2009) Inhibition of ATPase activity of *Escherichia coli* ATP synthase by polyphenols. *Int. J. Biol. Macromol.* **45**, 72–79.
- (51) Laughlin, T. F., and Ahmad, Z. (2010) Inhibition of *Escherichia coli* ATP synthase by amphibian antimicrobial peptides. *Int. J. Biol. Macromol.* **46**, 367–374.
- (52) Ahmad, Z., Ahmad, M., Okafor, F., Jones, J., Abunameh, A., Cheniya, R. P., and Kady, I. O. (2012) Effect of structural modulation of polyphenolic compounds on the inhibition of *Escherichia coli* ATP synthase. *Int. J. Biol. Macromol.* **50**, 476–486.
- (53) Ferguson, S. J., Lloyd, W. J., and Radda, G. K. (1975) The mitochondrial ATPase. Selective modification of a nitrogen residue in the β subunit. *Eur. J. Biochem.* **54**, 127–133.
- (54) Ferguson, S. J., Lloyd, W. J., Lyons, M. H., and Radda, G. K. (1975) The mitochondrial ATPase. Evidence for a single essential tyrosine residue. *Eur. J. Biochem.* **54**, 117–126.
- (55) Nadanaciva, S., Weber, J., and Senior, A. E. (2000) New probes of the F1-ATPase catalytic transition state reveal that two of the three

catalytic sites can assume a transition state conformation simultaneously. *Biochemistry* 39, 9583–9590.

(56) Nadanaciva, S., Weber, J., and Senior, A. E. (1999) Binding of the transition state analog MgADP-fluoroaluminate to F1-ATPase. *J. Biol. Chem.* 274, 7052–7058.

(57) Bowler, M. W., Montgomery, M. G., Leslie, A. G., and Walker, J. E. (2006) How azide inhibits ATP hydrolysis by the F-ATPases. *Proc. Natl. Acad. Sci. U.S.A.* 103, 8646–8649.

(58) Yoshida, M., Allison, W. S., Esch, F. S., and Futai, M. (1982) The specificity of carboxyl group modification during the inactivation of the *Escherichia coli* F1-ATPase with dicyclohexyl-[¹⁴C]carbodiimide. *J. Biol. Chem.* 257, 10033–10037.

(59) Hermolin, J., and Fillingame, R. H. (1989) H⁺-ATPase activity of *Escherichia coli* F1F0 is blocked after reaction of dicyclohexylcarbodiimide with a single proteolipid (subunit c) of the F0 complex. *J. Biol. Chem.* 264, 3896–3903.

(60) Adachi, K., Oiwa, K., Nishizaka, T., Furuike, S., Noji, H., Itoh, H., Yoshida, M., and Kinoshita, K., Jr. (2007) Coupling of rotation and catalysis in F₁-ATPase revealed by single-molecule imaging and manipulation. *Cell* 130, 309–321.

(61) Tomblin, G., Bartholomew, L., Giménez, K., Tyndall, G. A., and Senior, A. E. (2004) Synergy between conserved ABC signature Ser residues in P-glycoprotein catalysis. *J. Biol. Chem.* 279, 5363–5373.